

Figures S1–S8:

**Kristoffer TG Rigbolt, Mostafa Zarei, Adrian Sprenger,
Andrea C Becker, Britta Diedrich, Xun Huang,
Sven Eiselein, Anders R Kristensen, Christine Gretzmeier,
Jens S Andersen, Zhike Zi, and Jörn Dengjel**

**Characterization of early autophagy signaling
by quantitative phosphoproteomics**

Autophagy 2014; 10(2)

<http://dx.doi.org/10.4161/auto.26864>

www.landesbioscience.com/journals/autophagy/article/26864

Figure S1

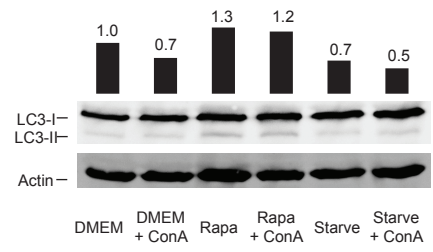


Figure S2

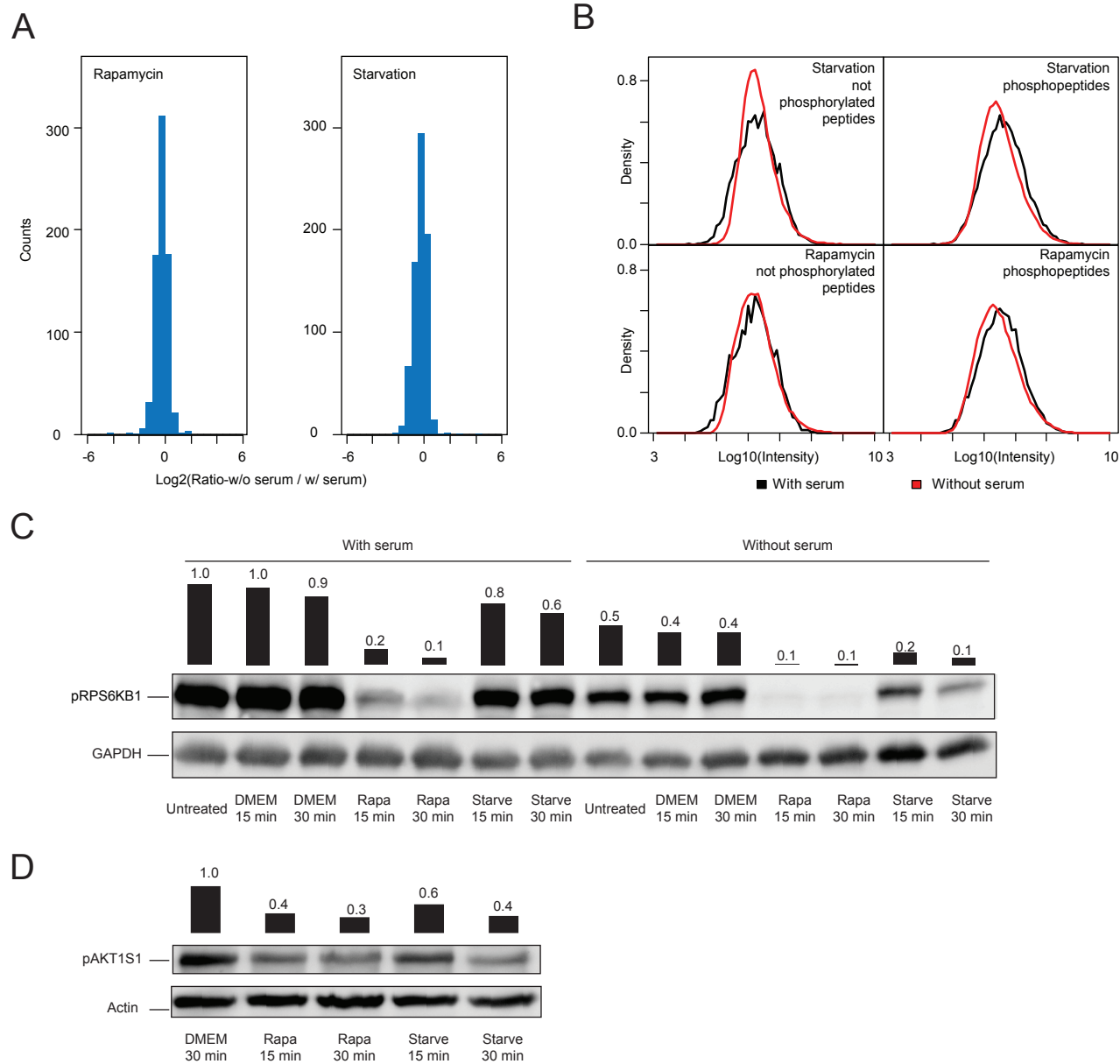
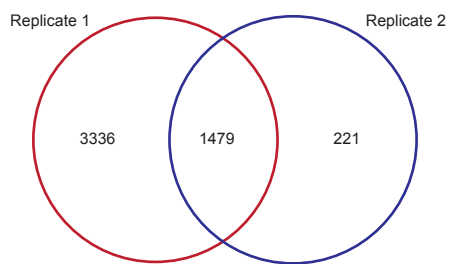
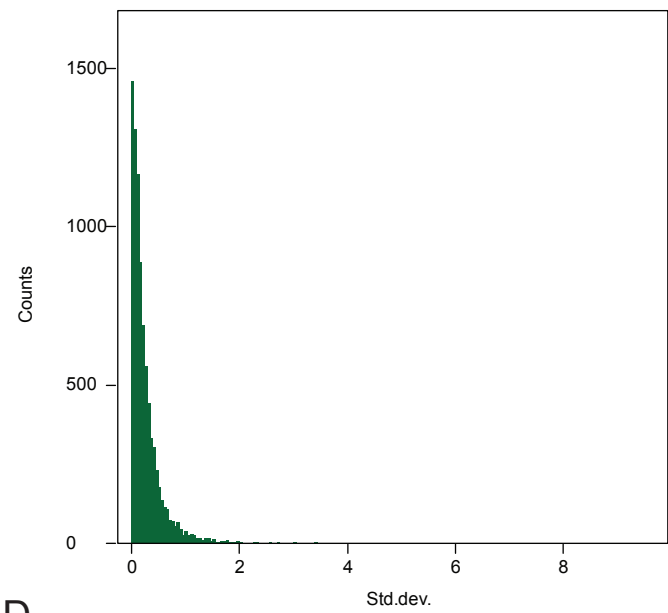


Figure S3

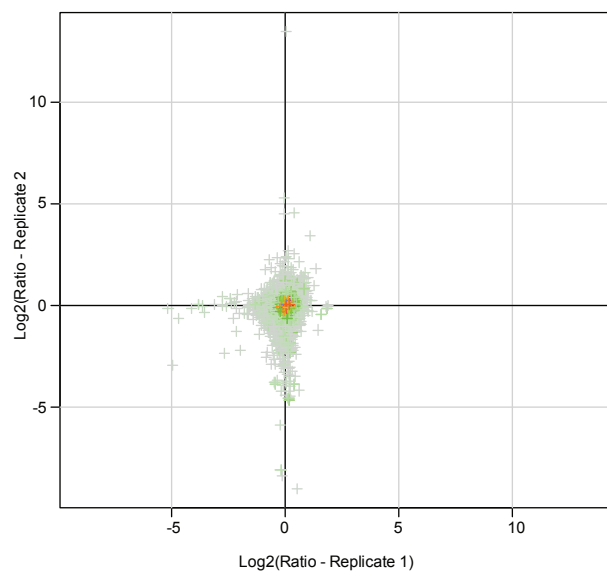
A



B



C



D

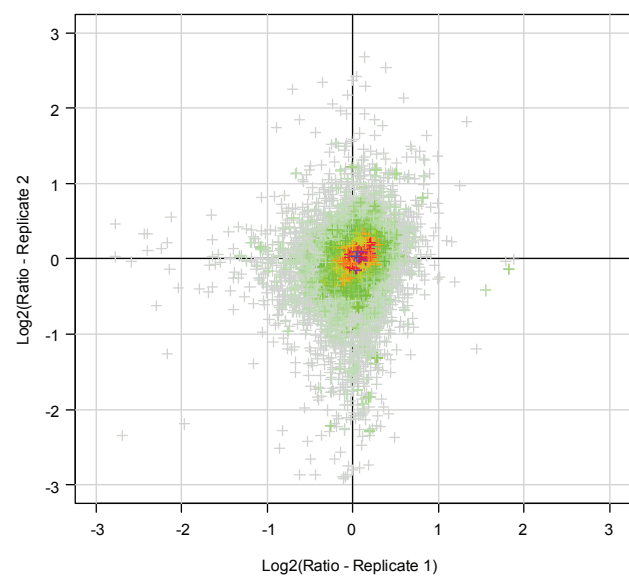


Figure S4

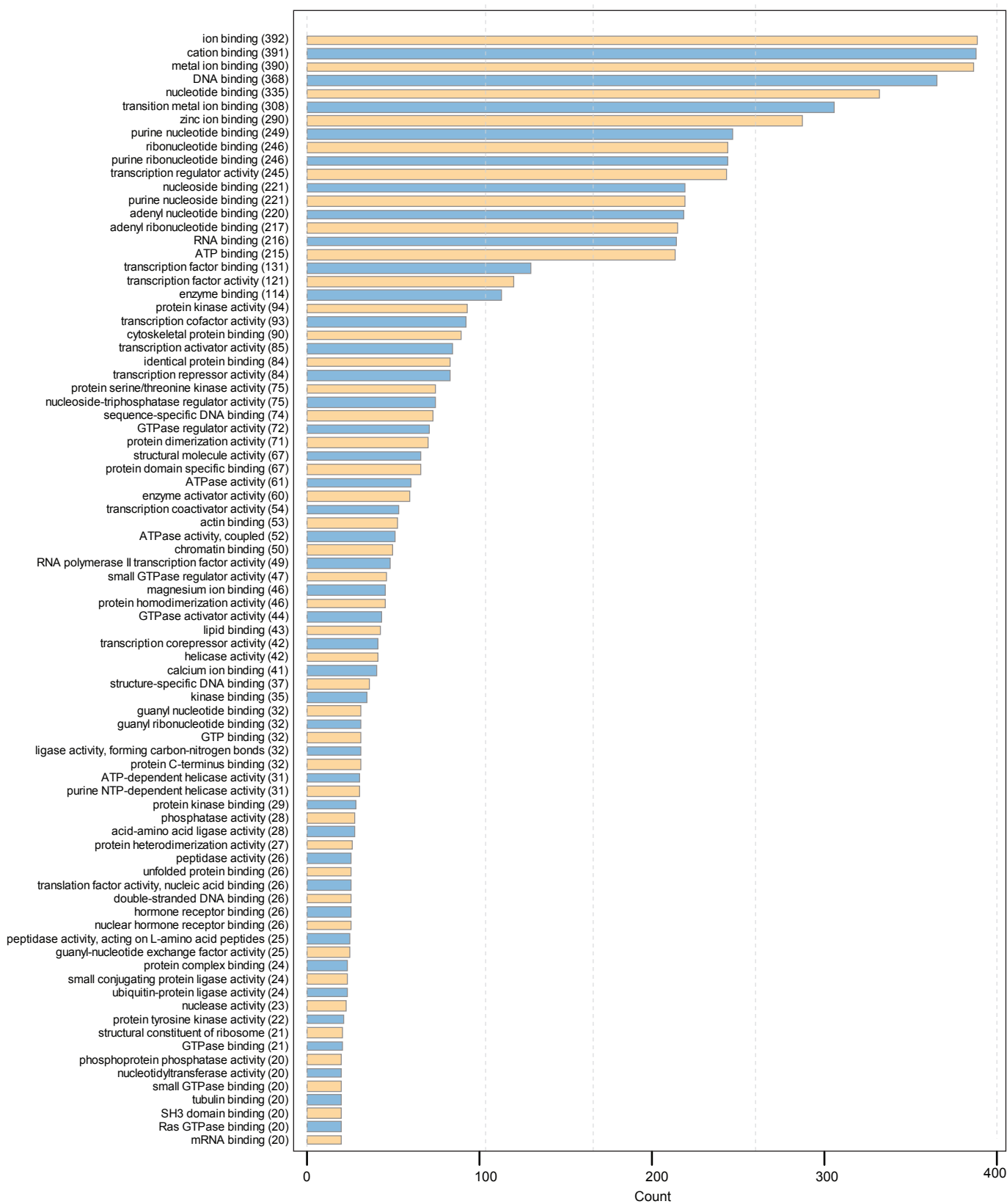
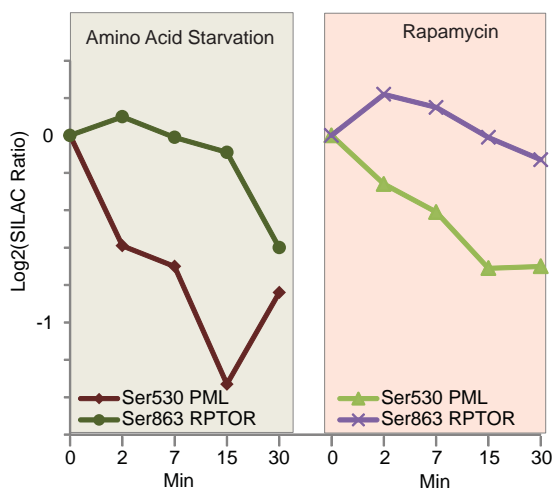
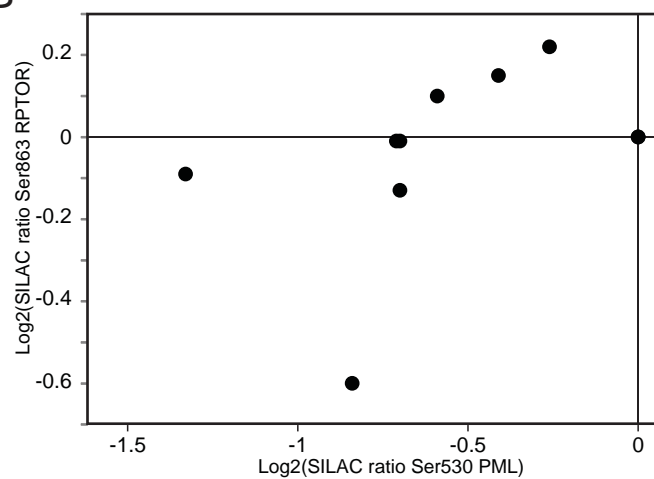


Figure S5

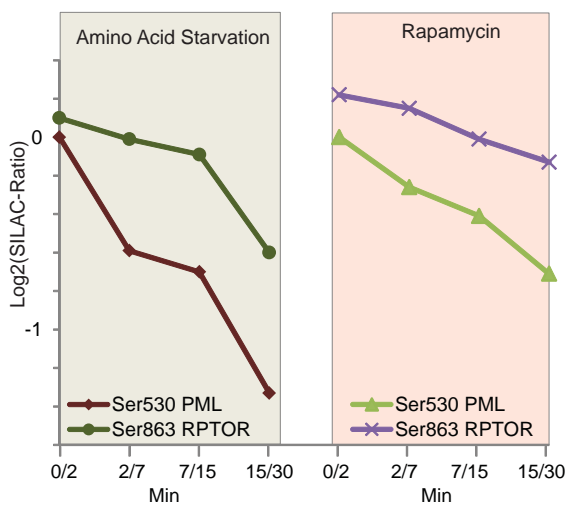
A



B



C



D

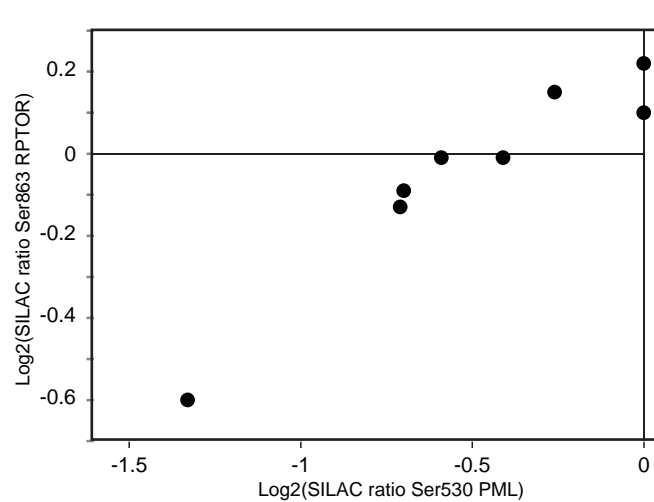
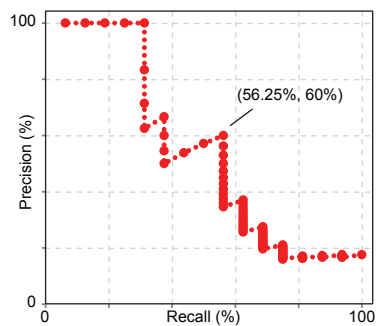


Figure S6

A



B

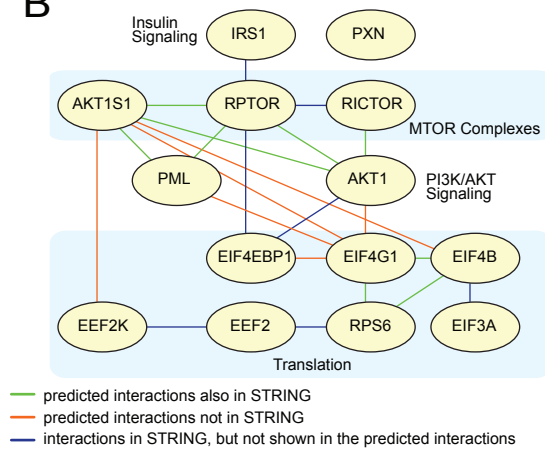


Figure S7

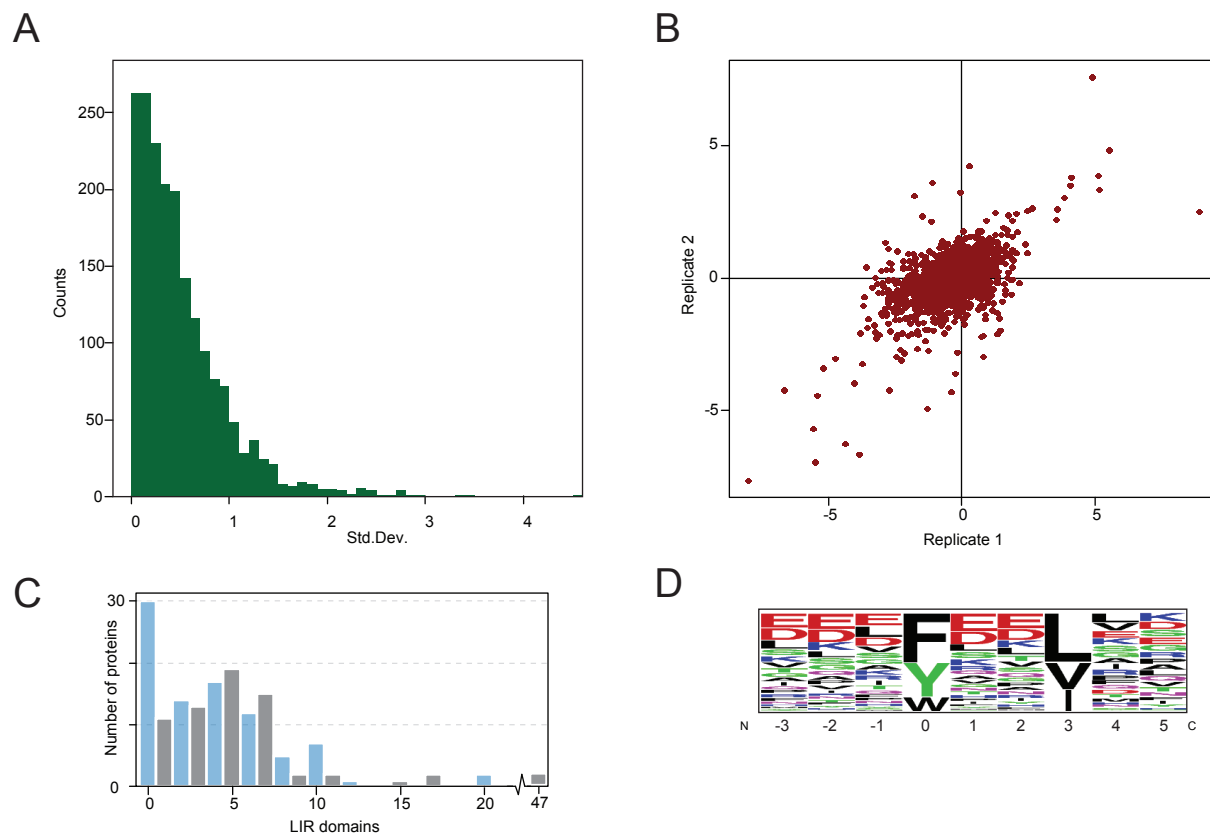


Figure S8

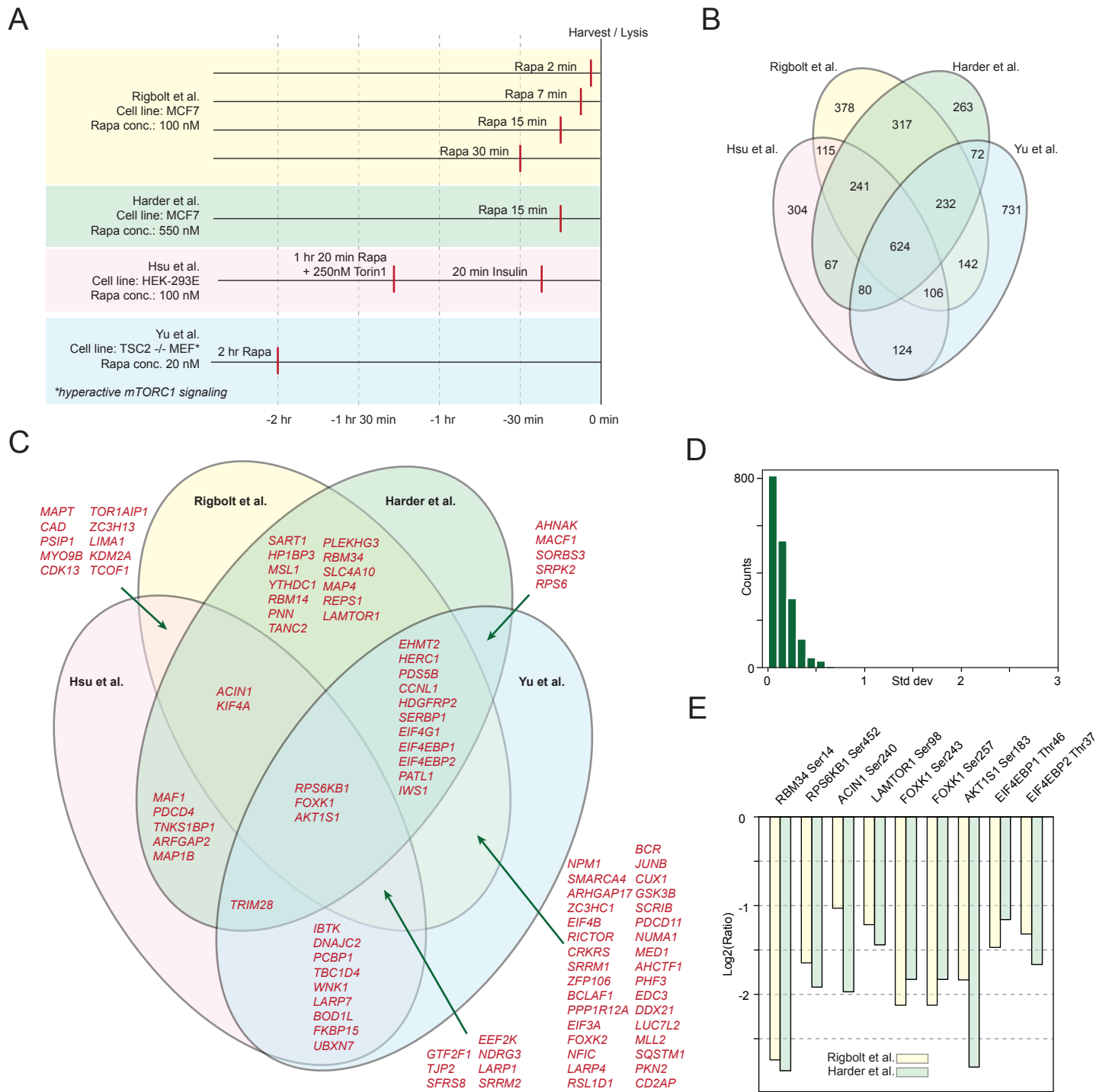


Figure S1. Analysis of LC3-II formation upon autophagy induction by rapamycin or starvation performed in dialyzed serum. Bars indicate quantitation of LC3-II normalized to Actin relative to the first lane.

Figure S2. Evaluation of the effect of serum starvation on the induction of autophagy.

(A) Using an experimental setup essentially identical to that used to acquire the data for temporal characterization by quantitative phosphoproteomics the response of the phosphoproteome to autophagy induction by starvation or rapamycin for 30 min of cells not serum-starved prior to induction was assayed. The histograms show the difference between the ratios obtained from experiments without and with serum for rapamycin (left) and starvation (right). A minimal effect on the ratios is observed as the vast majority cluster around the center, corresponding to no change. (B) Distribution of intensity values from MS analysis in (A). The intensity values for phosphopeptides were normalized by the difference in intensity of unphosphorylated peptides to account for differences due to technical issues. For the phosphopeptides it is noted that the intensities are lower in samples from serum-starved cells. (C) Western blot of Thr389 on RPS6KB1 in cells treated as indicated either with or without serum. Bars indicate quantitation normalized to GAPDH relative to the first lane. Serum starvation reduces phosphorylation levels preserving relative changes. (D) Western blot of Ser183 on AKT1S1 in cells treated as indicated with serum. Bars indicate quantitation normalized to actin relative to the first lane. Compare to figure 4F for influence of serum starvation.

Figure S3. Reproducibility of phosphorylation site quantifications. **(A)** Overlap of class 1 sites quantified in 2 biological replicates. 70 additional sites were identified but could not be quantified. **(B)** Standard deviation of ratios from 2 biological replicates. **(C)** Density scatter plot of ratios from replicates. **(D)** Zoom of the region $\pm 3 \text{ Log}_2(\text{SILAC})$ -ratio in **(C)**.

Figure S4. Graphical summary of the GO molecular function terms represented in the phosphorylation data retrieved from the DAVID resource. Only terms with more than 20 occurrences are shown, see Table S2 for a full list.

Figure S5. Principle of time-lagged correlation analysis. **(A)** When comparing the profiles of Ser530 PML and Ser863 RPTOR these are clearly different **(B)** and therefore a rather poor correlation with a Pearson coefficient of 0.42 is obtained. If the last time-point from the Ser530 PML profile (30 min) and the first time-point from the Ser863 RPTOR profile (0 min) are omitted, corresponding to displacing the profiles in respect to each other to account for a time lag the profiles are much more similar **(C)** and a better correlation is observed **(D)** with the Pearson coefficient of 0.95 indicating that the regulation of these sites are dependent with a time-lag.

Figure S6. Inference of protein-protein interactions of the MTOR signaling pathway proteins. **(A)** Precision-recall curve of the predicted interaction network, the coordinate of the optimal threshold point is indicated. **(B)** Overview of the inferred interaction network, predicted interactions present in STRING are indicated with green edges,

predicted interactions not in STRING in orange and blue edges indicate interactions in STRING not predicted by our inference.

Figure S7. Reproducibility of LC3-interaction screen quantifications and analysis of potential LIR motifs. **(A)** Standard deviation of ratios from 2 biological replicates. **(B)** Density scatter plot of ratios from replicates. **(C)** Number of LIR motifs in the sequence of significantly enriched LC3-interacting proteins. **(D)** Summary of the identified putative LIR motifs with F, Y or W in the 0 position and L, V or I in the 3 position.

Figure S8. Comparison of global studies of the MTOR-sensitive phosphoproteome. **(A)** Overview of the cell stimulation regime used by 4 independent studies. **(B)** Overlap of all identified phosphoproteins in the 4 studies outlined in **(A)**. **(C)** Subset of phosphoproteins in **(B)** which are rapamycin sensitive. **(D)** Standard deviation of phosphorylation-site ratios for sites identified both in this work and in Harder et al. (see accompanying manuscript in this issue). **(E)** Overview of phosphorylation-site ratios of sites identified as rapamycin sensitive by both this work and Harder et al.